Lifescience Global

Journal of Coating Science and Technology
http://www.lifesciencegloba l.com/journals/journal-of-coating-science-and-technology

PTFE-Doped CeO_2 Films: Synthesis, Characterization and Properties

Y. Taga*, K. Nishimura and Y. Hisamatsu

Thin-film Research Center, Chubu University, Kasugai, Japan

Abstract: Multi-functional hybrid films were developed by doping PTFE into CeO_2 by co-sputtering of CeO_2 and PTFE targets. The hybrid films formed on borosilicate glass substrate containing from 5 to 15 vol. % PTFE in CeO_2 showed UV shielding, high indentation hardness, hydrophobicity, optical transmittance in visible light, and high bending crack resistance. Optical properties of 100 nm thick CeO_2 -5 vol. % PTFE film revealed UV light shielding of more than 80 % at 380 nm and visible light transmittance higher than 80 %. Indentation hardness measured under the load of 0.001mN was more than 16,000N/mm^2 of 2.7 times higher than the glass substrate. No crack in the film was observed by bending 1.5 cm in diameter. Furthermore, the hydrophobic surface property was evaluated by the water contact angle to be higher than 90 degrees. Preliminary characterization of the CeO_2-PTFE film using XPS and XMA revealed that chemical states of F in sputter doped PTFE in CeO_2 can be considered to exist as C-F and Ce-F compounds. On the other hand, chemical states of Ce changed partially from Ce^{+4} (CeO_2) to Ce^{+3} (Ce_2O_3 or CeF_3) with increasing doped PTFEF in the film.

In this rapid communication, we preliminary described the optical, mechanical and chemical properties of newly developed hybrid CeO_2-PTFE films prepared by sputtering.

Received on 16-11-2019
Accepted on 31-12-2019
Published on 08-01-2020

Keywords: Hybrid sputtering films, CeO_2-PTFE film, Super-hard, UV shieldinng, Water repellamt, Bending rsistance, Transparent in visible light, PTFE doping, XPS, Nanoindentor.

DOI: https://doi.org/10.6000/2369-3355.2019.06.02.1

Cubic bulk material of CeO_2 has been attracting great attention as one of the most promising materials from the viewpoints of optical and heat-resisting properties, toughness against mechanical abrasion, and even chemical attack. CeO_2 was inevitably micronized into nanoparticles to develop for a wide range of catalytic applications [1]. Furthermore, film formation of CeO_2 was soon carried out by various methods and tried to apply optical coatings [2], heterogeneous catalysts [3-7]. As is well known, thin film properties are strongly influenced by their structure, composition and chemical bonding states of the constituent elements arising from preparation methods such as chemical vapour, physical vapour, and sol-gel depositions. Further improvement of the film properties was carried out by hybridization of the film with other elements by adjusting the structure and composition of starting material in chemical methods [8] or by doping in the physical process of thin-film formation [9].

To widen the application range of CeO_2 films, doping technology of other elements is one of the most useful methods not only for materials search of CeO_2-based hybrid thin film but also for basic research of materials science. Until today, various metal cations have been doped into CeO_2 with a special interest in catalysis [10-12] but there exist only a few reports of anion doping [13-15] in spite of their interesting applications such as oxygen barrier coatings for food package and water repellent coating [16, 17]. Ce is also well known to exist +4 in the oxidation state of CeO_2, but the valence changes to +3 in fluoride state of CeF_3, where highly electronegative fluoride ions were formed. Therefore, CeO_2 can incorporate fluoride ion, resulting in a change of Ce^{3+}/Ce^{+4} redox couple. In spite of many basic research reports of CeO_2-based hybrid thin films, there exists no report on thin-film performances such as optical, mechanical and chemical properties for practical applications. We described first of all the optical, mechanical and chemical properties of PTFE doped CeO_2 films prepared by co-sputtering of CeO_2 and PTFE targets.

Doping of PTFE into CeO_2 was carried out by radio-frequency magnetron sputtering method under the conditions shown in Table **1**. Composition of doped PTFE was determined by the concentration of F in the film determined by EPMA (Electron Probe Micro Analyzer JXA-8530F), where concentration ratio F/ (Ce + F) in vol. % in hybrid film was used in this paper.

Figure **1** showed the optical transmittance of CeO2-PTFE films with 80 -100 nm thick with the light wavelength from

*Thin-film Research Center, Chubu University, Kasugai, Japan; Tel: +81-568-51-9819; Fax: +81-568-51-9098; E-mail: y-taga@isc.chubu.ac.jp

E-ISSN: 2369-3355/19

Table 1: Sputter Doping Conditions of PTFE into CeO_2 Films

Parameters	Conditions
Targets	Sintered CeO_2, PTFE
Dimension of targets	76.2 mm in diameter and 5 mm in thickness
Substrate	0.7 mm thick borosilicate glass
Working gas and pressure	Argon at 1Pa
RF magnetron ower	200W for CeO_2 and 20-50W for PTFE
Deposition rate	4~5 nm/min
Deposition time	20 min
Film thickness	80 -100 nm
Distance between target to substrate	5 cm

250nm to 2500nm was evaluated by using Hitachi 4100 spectrometer and deposition rate and film thickness by a laser microscope (Keyence VK-X210/200) using a 408 nm visible light. Composition and structure of the hybrid films were analyzed by EPMA and thin-film XRD (Rigaku ATX-E), respectively. UV light-shielding properties were usually evaluated the transmittance at the wavelength of 380 nm. CeO_2 film showed a typical UV shielding properties, where threshold wavelength 330 nm of UV shielding corresponds to band gap E g of 3.4 eV, which was large compared to bulk CeO_2 of 3.1-3.2 eV. This difference can be explained by the bandgap widening by the non-equilibrium state of as-sputtered film CeO_{2-X} film. Threshold wavelength of sputtered CeO_2-PTFE films remains unchanged up to 15 vol.% but drastic change can be seen over 20 vol.%, where UV shielding properties disappeared by the change of band structure of CeO_2. Characterization of CeO_2-PTFE films was carried out by X-ray photoelectron spectroscopy (XPS) to elucidate the chemical states of the films. At first, a typical XPS core-level spectrum of C_{1s} in PTFE film sputter-deposited by argon gas recorded using Mg radiation (photon energy = 1253.6 eV) as shown in Figure **2**, where XPS spectrum of C1s of thermally evaporated PTFE film is also shown in the figure by a dotted line for reference. The core-level spectra of the sputter-deposited film were fitted after adjusting the baseline relative to signal background. The chemically distinct species of functional groups were also resolved using Gaussian distribution fitting procedure with the peak positions and area were determined. The C_{1s} core-level spectra at binding energy E_b at 284.6 eV were taken as reference for charge correction in the core-level spectra, and the peak position was calibrated with respect to it. Functional groups of C_{1s} spectra of PTFE film were assigned as follows [18]: C-C at 284.6 eV, C-CF_x at 288.0 eV, CF at 290.0 eV, CF_2 at 292.7 eV and CF_3 at 294.5 eV.

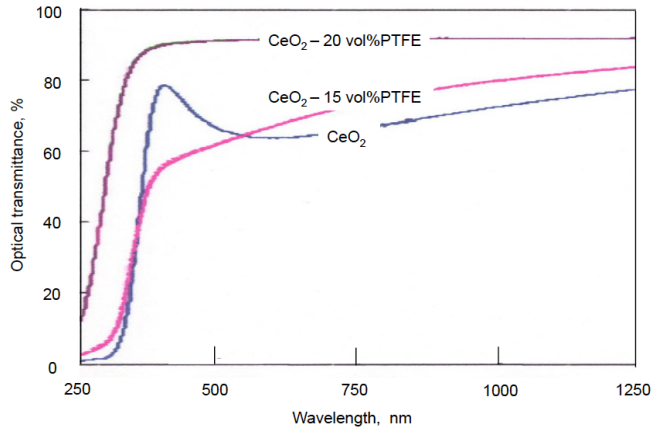

Figure 1: Optical transmittance of CeO_2-PTFE hybrid films.

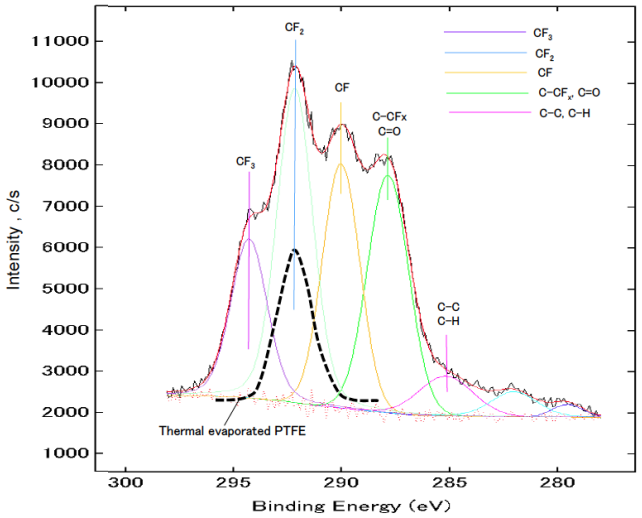

Figure 2: C1s XPS spectra of sputtered PTFE films.

The core-level spectra of C_{1s}, Ce_{3d}, F_{1s} of CeO_2-PTFE hybrid films and sputtered CeF_3 film were shown in Figure **3**. Functional groups [19] of C-O, C-O-H (Ether and alcohol), C=O (Carbonyl), C=O-O (Ester, Acid), C=O-O-O (Carbonate), C=O-O-OH (Carboxyl) and small amount of functional groups of C-F_x increased by doping PTFE up to 15 vol.% but further addition of PTFE results in large emerging peaks of C-F_x functional groups appeared at E_b from 290eV to 295eV [6, 8, 19]. These results indicated that sputter doped PTFE was found to exist in the forms of C-F_x, which may give hydrophobic surface properties [19, 20]. Typical Ce_{3d} spectra were observed from CeO_2 films with satellite

peak at 918 eV indicating Ce^{+4} chemical state and of course, no fluorine was detected. With the increase in PTFE content in CeO_2 films, C_{3d} spectra indicated a gradual change in chemical sates of Ce from Ce^{+4} to Ce^{+3} as assigned in the figure and the satellite peak at 918 eV decreased accordingly. Besides, large functional groups at E_b from 290eV to 295eV also indicated the formation of CeF_3 in hybrid films. However, F_{1s} peaks remain unchanged even by doping PTFE up to 20 vol.% of PTFE, indicating that fluorine in CeO_2-PTFE hybrid films exists in the same chemical states of CeF_3 but not different from PTFE as shown in Figure **4** (F_{1s} in PTFE at 689 eV and in CeF_3 at 685 eV).

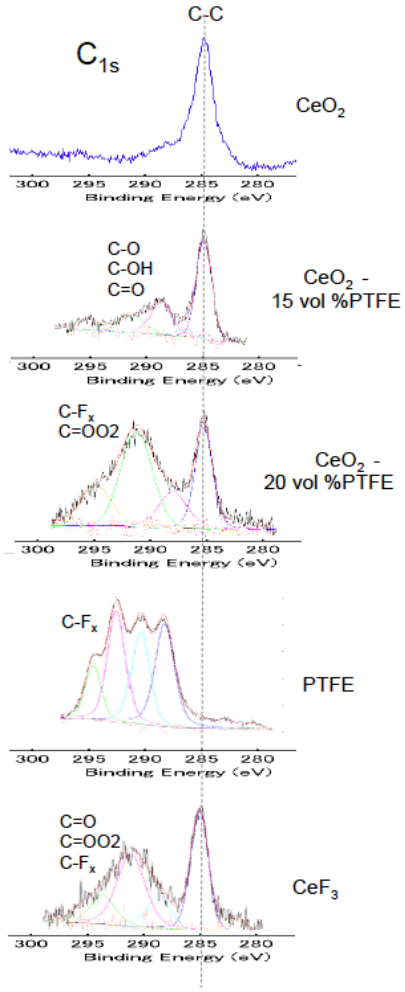

Figure 3: Change in C1s spectra in CeO_2-PTFE hybrid films and bulk PTFE and CeF_3.

C-F_X BONDS IN CHEMICAL COMPOUNDS

Based on the XPS analyses shown in Figures **3** and **4**, we can conclude that chemical states of fluorine of sputter doped PTFE in CeO_2 can be considered to exist as CeF3 and C-F_x and the host element of Ce changed partially from Ce^{+4} (CeO_2) to Ce^{+3} indicating the formation of Ce_2O_3 or CeF_3.

According to the basic process of sputtering [21], the constituent elements of the targets made of metals and ceramics will leave target surface to the substrate in the form of the atomic particle by momentum transfer from sputtering working gas atoms to the target. Therefore, CeO_2 target was considered to be sputtered in atomic Ce and atomic O, but there exists no report on the form of sputtered particles of polymer target such as PTFE. Experimental results shown in Figure **2** revealed that PTFE was sputtered mainly in the form of C-F_2 from the target to deposit on the substrate as a physical mixture of C, F, CF, CF2 and CF3. As a result, film growth by sputtering of CeO_2-PTFE target can be considered by chemical reaction on the substrate among co-landing atomic Ce, O, C from CeO_2 target and C, F, CF, CF2 and CF3 from PTFE target.

Degree of indentation hardness (IH) of bulk substrates and CeO_2-PTFE hybrid films was evaluated using Nano Indenter (Nanomechanics i Micro) under the load of 0.001mN. As shown in Figure **5**, IH of borosilicate glass substrate about 6,364 N/mm^2 increased steeply to over 20,876 N/mm^2 by sputter deposition of 100 nm thick CeO_2 film and then decreased gradually by doping of PTFE in CeO_2 up to 20 vol.%. IH of CeO_2-PTFE hybrid films on borosilicate glass substrate was found to be over 10,000 N/mm^2 even up to 20 vol.%PTFE in CeO_2. It can be understood that IH of CeO_2 film is a reflection of the hardness of bulk CeO_2 which is widely known as a grinding abrasive. Furthermore, IH of over 820 N/mm^2 of sputtered PTFE films compared to IH of 33 N/mm^2 of bulk PTFE substrate can be explained in terms of sputter induced polymerization of PTFE films [18]. It is very interesting to note that CeO_2-PTFE hybrid films containing PTFE from 0 to 15vol.% showing excellent UV shielding properties showed super IH from 15,000 to 20,000 N/mm^2 at the same time.

Hydrophilic/hydrophilic property was evaluated by contact angle measurement of water droplet of 1 μL using Drop master 500 System of Kyowa Interface Science. All samples were found to be more than 90 degrees after annealing at 100℃ shown in Figure **6**. Film surfaces showed water repellant properties and the contact angle of more than 90 degrees in composition range from 5 to 30 vol. %PTFE in CeO_2. Hydrophobic properties of CeO_2-PTFE films thus obtained may be due to the effect of the hydrophobic additive of PTFE and spontaneous water repellency of sputtered CeO_2 films [22].

In conclusion, multi-functional hybrid films were developed by doping PTFE into CeO_2 by sputter deposition using CeO_2 and PTFE targets. Hybrid films containing from 5 to 15 vol.% PTFE in CeO_2 showed 4 functions of UV shielding, super indentation hardness, hydrophobicity and optical transmittance in visible light. Detailed investigation of surface properties using XPS and EPMA revealed that chemical states of F of sputter doped PTFE in CeO_2 can be considered to exist as C-F_x and the host element of Ce changed correspondingly from Ce^{+4} (CeO_2) to Ce^{+3} indicating the formation of Ce_2O_3 or CeF_3. Furthermore, hydrophobic surface properties can be also explained in terms of surface

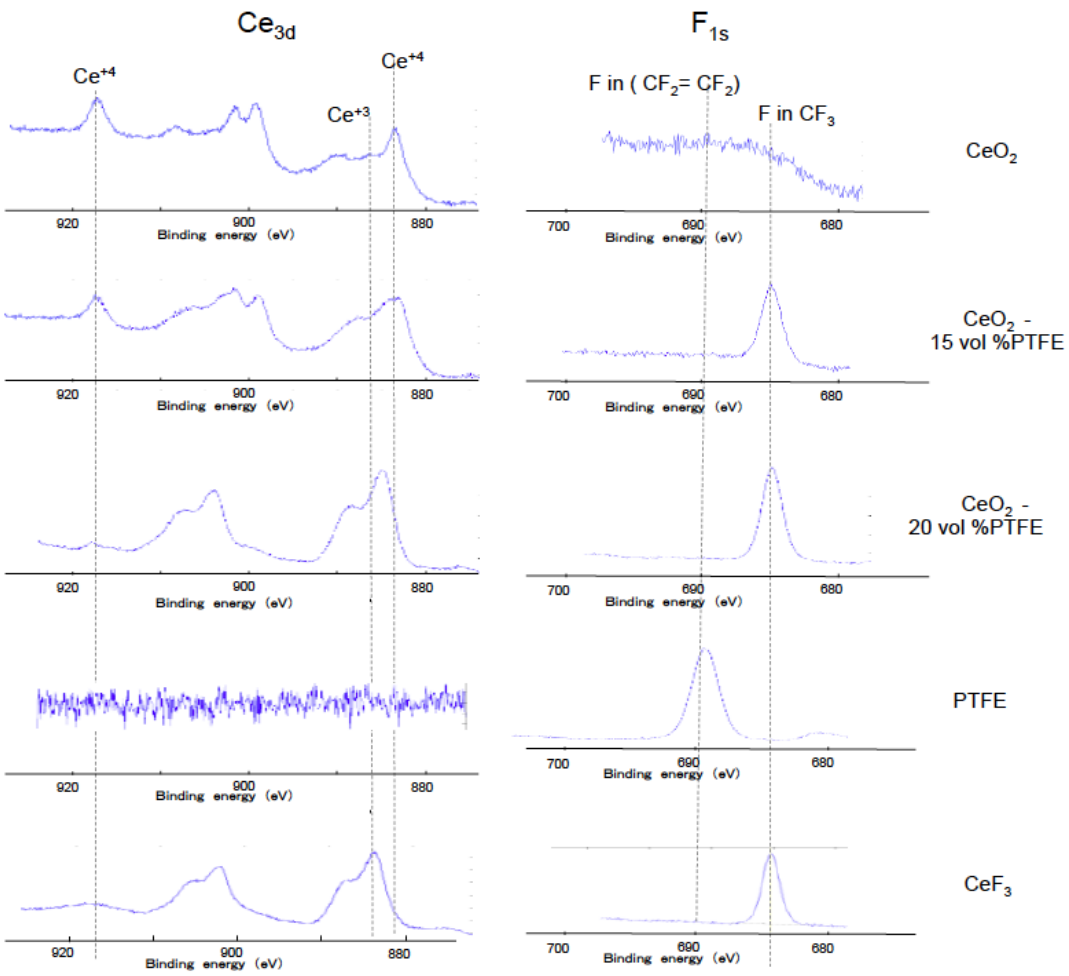

Figure 4: Change in Ce3d and F1s spectra in CeO_2-PTFE hybrid films and bulk PTFE and CeF_3.

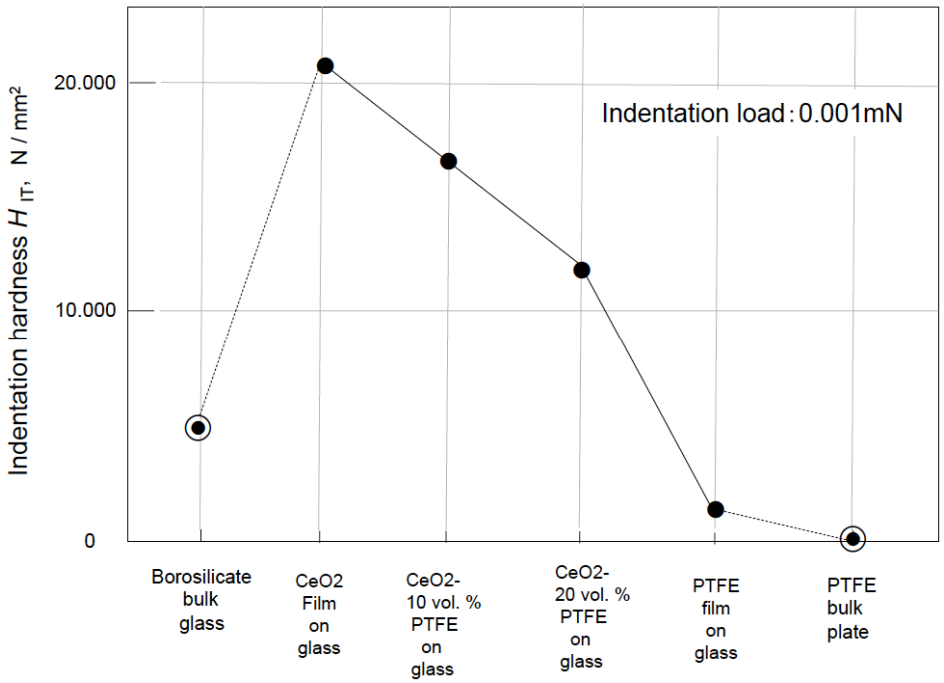

Figure 5: Changes in indentation hardness of CeO_2-PTFE hybrid films on borosilicate glass and PTFE.

concentration of F of CeO_2-PTFE films evaluated by XPS analyses.

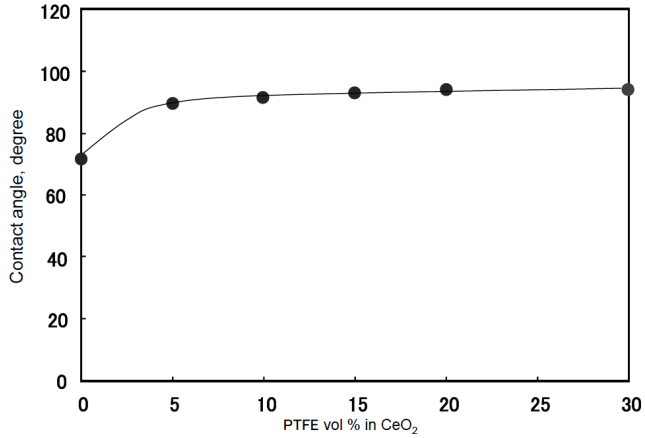

Figure 6: Changes in contact angle with film composition.

REFERENCES

[1] Montini T, Melchionna M, Monai M, Fornsiero P. Fundamentals and catalytic applications of CeO_2-based materials. Chem Rev 2016; 116: 5987-6041. https://doi.org/10.1021/acs.chemrev.5b00603

[2] Netterfield RP, Saintry WG, Martin PJ, Sie SH. Properties of CeO_2 thin films prepared by oxygen-ion-assisted deposition. Appl Optics 1985; 24: 2267-2272. https://doi.org/10.1364/AO.24.002267

[3] Toro RG, Malandrino G, Fragala IL, Nigro RL, Losurdo M, Buruno G. Relationship between the nanostructures and the optical properties of CeO_2 thin films. J Phys Chem B 2004; 108: 16357-16364. https://doi.org/10.1021/jp048083j

[4] Murray EP, Tsai T, Barnett SA. A direct-methane fuel cell with a ceria-based anode. Nature 1999; 400: 649-651. https://doi.org/10.1038/23220

[5] Fu Q, Saltsburg H, Flytzani-Stephanopoulos M. Active nonmetallic Au and Pt species on ceria-based water-gas shift catalysts. Science 2003; 301: 935-938. https://doi.org/10.1126/science.1085721

[6] Singh P, Hegde MS. Controlled synthesis of nanocrystalline CeO_2 and $Ce_{1-x}MxO_2$−δ (M=Zr, Y, Ti, Pr and Fe) solid solutions by the hydrothermal method: Structure and oxygen storage capacity. J Solid State Chem 2008; 181: 3248-3256. https://doi.org/10.1016/j.jssc.2008.08.018

[7] Paier J, Penschke C, Sauer J. Oxygen defects and surface chemistry of ceria: quantum chemical studies compared to experiment. Chem Rev 2013; 113: 3949-3985. https://doi.org/10.1021/cr3004949

[8] Mullins DR. The surface chemistry of cerium oxide. Surf Scie Rep 2015; 70: 42. https://doi.org/10.1016/j.surfrep.2014.12.001

[9] Asahi R, Morikawa T, Ohwaki T, Aoki K, Taga Y. Visible-light photocatalysis in nitrogen-doped titanium oxides Science 2001; 293: 269-271. https://doi.org/10.1126/science.1061051

[10] Mogensen M, Linegaraard T, Hansen UR, Mogensen G. Physical properties of mixed conductor solid oxide fuel cell anodes of doped CeO_2. J Electrochem Soc 1994; 141: 2122-2128. https://doi.org/10.1149/1.2055072

[11] Yashiro H, Eguchi Y, Eguchi K, Arai H. Oxygen ion conductivity of the ceria-samarium oxide system with fluorite structure. J Appl Electrochem 1988; 18: 527-531. https://doi.org/10.1007/BF01022246

[12] Wang DY, Park DS, Griffith J, Nowick AS. Oxygen-ion conductivity and defect interactions in yttria-doped ceria. Solid State Ionics 1981; 2: 95-105. https://doi.org/10.1016/0167-2738(81)90005-9

[13] Jorge AB, Sakatani Y, Boissiere C, Laberty-Roberts C, Sauthier G, Fraxedas J, Sanchez C, Fuertes A. Nanocrystalline N-doped ceria porous thin films as efficient visible-active photocatalysts. J Mater Chem 2012; 22: 3220-3226. https://doi.org/10.1039/c2jm15230d

[14] Sun D, Gu M, Li R, Yin S, Song X, Zhao B, Li C, Feng Z, Sato T. Effects of nitrogen content in monocrystalline nano-CeO_2 on the degradation of dye in indoor lighting. Appl Surf Sci 2013; 280: 693-697. https://doi.org/10.1016/j.apsusc.2013.05.044

[15] Mao C, Zhao Y, Qui X, Zhu J, Burda C. Synthesis, characterization and computational study of nitrogen-doped CeO_2 nanoparticles with visible-light activity. Phys Chem Chem Phys 2008; 10: 5633-5638. https://doi.org/10.1039/b805915b

[16] Yabe S, Sato T. Cerium oxide for sunscreen cosmetics. J Solid State Chem Chem Mater 2003; 171: 7-11. https://doi.org/10.1016/S0022-4596(02)00139-1

[17] Zholobak NM, Ivanov VK, Shcherbakov AB, Shaporev AF, Polezhaeva OS, Baranchikov AY, Spivak NY, Tretyakov YD. UV-shielding property, photocatalytic activity and photocytotoxicity of ceria colloid solutions. J Photochem Photobiol B 2011; 102: 32-38. https://doi.org/10.1016/j.jphotobiol.2010.09.002

[18] Choukourov A, Pihosh Y, Stelmashuk V, Biederman H, Slavinska D, Kormund M, Zajickova L. Rf sputtering of composite SiO_x/plasma polymer films and their basic properties. Surface and Coatings Technology 2002; 151-152: 214-217. https://doi.org/10.1016/S0257-8972(01)01622-X

[19] Wolf MJ, Kullgren J, Boroqvist P, Hermasson K. Fluorine impurities at CeO_2(111): Effects on oxygen vacancy formation, molecular adsorption, and surface re-oxidation. J Chem Phys 2017; 146: 044703. https://doi.org/10.1063/1.4973239

[20] Kettner M, Sevcikova K, Homola P, Matolin V, Nehasil V. Influence of the Ce–F interaction on cerium photoelectron spectra in CeO_XF_Y layers. Chem Phys Lett 2015; 639: 126. https://doi.org/10.1016/j.cplett.2015.09.018

[21] Taga Y, Takahashi R. Role of kinetic energy of sputtered particles in thin film formation. Surface Sci 1997; 386: 231-240. https://doi.org/10.1016/S0039-6028(97)00313-0

[22] Taga Y, Ohwaki T. Hydrophobic surface treatment of metal oxides. Surface Technology 1996; 47: 571-574. https://doi.org/10.4139/sfj.47.571